

SELF-CALIBRATION OF GRAVITATIONAL SHEAR-GALAXY INTRINSIC ELLIPTICITY CORRELATION IN WEAK LENSING SURVEYS

PENGJIE ZHANG

Key Laboratory for Research in Galaxies and Cosmology, Shanghai Astronomical Observatory, Nandan Road 80, Shanghai, 200030, China

Draft version October 31, 2018

ABSTRACT

The galaxy intrinsic alignment is a severe challenge to precision cosmic shear measurement. We propose to self-calibrate the induced gravitational shear-galaxy intrinsic ellipticity correlation (the GI correlation, Hirata & Seljak 2004) in weak lensing surveys with photometric redshift measurement. (1) We propose a method to extract the intrinsic ellipticity-galaxy density cross correlation (I-g) from the galaxy ellipticity-density measurement in the same redshift bin. (2) We also find a generic scaling relation to convert the extracted I-g correlation to the demanded GI correlation. We perform concept study under simplified conditions and demonstrate its capability to significantly reduce the GI contamination. We discuss the impact of various complexities on the two key ingredients of the self-calibration technique, namely the method to extract the I-g correlation and the scaling relation between the I-g and the GI correlation. We expect none of them is likely able to completely invalidate the proposed self-calibration technique.

Subject headings: cosmology: gravitational lensing—theory: large scale structure

1. INTRODUCTION

Weak gravitational lensing is one of the most powerful probes of the dark universe (Refregier 2003; Albrecht et al. 2006; Munshi et al. 2008; Hoekstra & Jain 2008). It is rich in physics and contains tremendous information on dark matter, dark energy and the nature of gravity at large scales. Its modeling is relatively clean. At the multipole $\ell < 2000$, gravity is the dominant force shaping the weak lensing power spectrum while complicated gas physics only affects the lensing power spectrum at less than 1% level (White 2004; Zhan & Knox 2004; Jing et al. 2006; Rudd et al. 2008). This makes the weak lensing precision modeling feasible, through high precision simulations. On the other hand, weak lensing has been measured with high significance. The most sophisticated method so far is to measure the cosmic shear, lensing induced galaxy shape distortion. After the first detections in the year 2000 (Bacon et al. 2000; Kaiser et al. 2000; Van Waerbeke et al. 2000; Wittman et al. 2000), data quality has been improved dramatically (e.g. Fu et al. 2008).

However, it is still challenging to perform precision lensing measurement. A potentially severe problem is the non-random galaxy intrinsic ellipticity (intrinsic alignment). Its existence is supported by many evidences. Angular momentum of dark matter halos is influenced by the tidal force of the large scale structure. More importantly, mass accretion is more preferentially along the filaments (e.g. Zhang et al. 2009). This causes the dark matter halo ellipticities (and also halo orientations) to be correlated over tens of Mpc (Croft & Metzler 2000; Heavens et al. 2000; Lee & Pen 2000; Catelan et al. 2001; Crittenden et al. 2001; Jing 2002; Zhang et al. 2009). Although galaxies are not perfectly aligned with the halo angular mo-

mentum vector, with the halo shape, or with each other (Heymans et al. 2004; Yang et al. 2006; Kang et al. 2007; Okumura et al. 2008; Wang et al. 2008), the resulting correlations in galaxy spin (Pen et al. 2000) and ellipticity (Brown et al. 2002; Mackey et al. 2002; Heymans et al. 2004; Hirata et al. 2004; Lee & Pen 2007; Okumura et al. 2008; Schneider & Bridle 2009) are still measurable and contaminate cosmic shear measurement, especially for elliptical galaxies.

The intrinsic alignment biases the cosmic shear measurement. It introduces an intrinsic ellipticity-intrinsic ellipticity correlation (the II correlation). Since this correlation only exists at small physical separation and hence small line-of-sight separation, it can be effectively eliminated by the lensing tomography technique (King & Schneider 2002, 2003; Heymans & Heavens 2003), with moderate loss of cosmological information (Takada & White 2004).

However, as pointed out by Hirata & Seljak (2004) and then confirmed by observations (Mandelbaum et al. 2006; Hirata et al. 2007; Okumura & Jing 2009), the galaxy intrinsic ellipticity is also correlated with the large scale structure and thus induces the gravitational (cosmic) shear-intrinsic ellipticity correlation (the GI correlation). This contamination could bias the cosmic shear measurement at 10% level and dark energy constraints at more significant level (Bridle & King 2007). For this reason, there are intensive efforts to correct the GI contamination (e.g. Hirata & Seljak 2004; Heymans et al. 2006; Joachimi & Schneider 2008, 2009; Okumura & Jing 2009; Joachimi & Bridle 2009; Shi et al. 2010).

This paper proposed a new method to alleviate this problem. It is known that weak lensing surveys contains information other than the ellipticity-ellipticity correlation (e.g. Hu & Jain (2004); Bernstein (2009)). These information not only helps improve cosmological constraints, but also helps reduce errors in lens-

ing measurements, such as photometric redshift errors (Schneider et al. 2006; Zhang et al. 2009). We show that these extra information allows for a promising self-calibration of the GI contamination. The self-calibration technique we propose relies on no assumptions on the intrinsic ellipticity nor expensive spectroscopic redshift measurements.¹ It is thus applicable to ongoing or proposed lensing surveys like CFHTLS, DES, Euclid, LSST and SNAP/JDEM. Under simplified conditions, we estimate the performance of this technique and its robustness against various sources of error. We find that it has the potential to reduce the GI contamination significantly.

The paper is organized as follows. In §2, we explain the basic idea of the self-calibration technique. We investigate the self-calibration performance in §3, discuss extra sources of error in §4 and summarize in §5. We leave some technical details in the appendices §A, B & C.

2. A SIMPLIFIED VERSION OF THE GI SELF-CALIBRATION

In the section, we present the basic idea of the self-calibration technique. To highlight the key ingredients of this technique, we adopt a simplified picture and neglect many complexities until §3 & §4.

2.1. The information budget in weak lensing surveys

In lensing surveys, we have several pieces of information (refer to Bernstein (2009) for a comprehensive review). What relevant for the self-calibration technique is the shape, angular position and photometric redshift of each galaxy. Only galaxies sufficiently large and bright are suitable for cosmic shear measurement. To avoid possible sample bias, we will restrict the discussion to this sub-sample. We split galaxies into a set of photo-z bins according to their photo-z z^P . The i -th bin has $\bar{z}_i - \Delta z_i/2 \leq z^P \leq \bar{z}_i + \Delta z_i/2$. Our convention is that, if $i < j$, then $\bar{z}_i < \bar{z}_j$. $\bar{n}_i^P(z^P)$ and $\bar{n}_i(z)$ are the mean galaxy distribution over the i -th redshift bin, as a function of photo-z z^P and true redshift z respectively. The two are related by the photo-z probability distribution function (PDF) $p(z|z^P)$. Intrinsic fluctuations in the 3D galaxy distribution, δ_g , cause fluctuations in the galaxy surface density of a photo-z bin, δ_Σ . This is one piece of information in weak lensing surveys.

The galaxy shape, expressed in the term of ellipticity, measures the cosmic shear $\gamma_{1,2}$ induced by gravitational lensing. For each galaxy, this signal is overwhelmed by galaxy intrinsic ellipticity. If galaxy intrinsic ellipticity is randomly distributed, it only causes shot noise in the cosmic shear measurement, which is straightforward to correct. For this reason, we will not explicitly show this term in relevant equations, although we do take it into account in the error estimation. However, gravitational tidal force induces correlations in ellipticities of close galaxy pairs. For this, the measured shear $\gamma_{1,2}^s = \gamma_{1,2} + I_{1,2}$,

¹ We still need sufficiently accurate photo-z, which controls the I-g measurement error §3.1 and the accuracy of the scaling relation (§3.3). Since photo-z algorithm relies on calibration against spectroscopic samples (not necessarily of the same survey), in this sense, our self-calibration does rely on spectroscopic redshift measurements.

where I denotes the correlated part of the galaxy intrinsic ellipticity and 1, 2 denote the two components of the cosmic shear and the intrinsic alignment. $\gamma_{1,2}$ describe the shape distortion along the x-y axis and the direction of 45° away, respectively. γ is equivalent to the lensing convergence κ (in Fourier space, this relation is local). Thus we will work on κ instead of $\gamma_{1,2}$. From the measured γ^s , we obtain $\kappa^s = \kappa + I$. Here, I is the E mode of $I_{1,2}$, analogous to κ , which is the E mode of $\gamma_{1,2}$ (Stebbins 1996; Crittenden et al. 2002). Although cosmic shear, to a good approximation, does not have B-mode, the intrinsic alignment can have non-vanishing B-mode (e.g. Hirata & Seljak 2004; Schneider & Bridle 2009). This piece of information is useful to diagnose and hence calibrate the intrinsic alignment. However in the current paper, we will focus on the E-mode.

κ is the projection of the matter over-density along the line of sight. For a flat universe and under the Born approximation, the lensing convergence κ of a galaxy (source) at redshift z_G and direction $\hat{\theta}$ (Refregier 2003) is

$$\kappa(\hat{\theta}) = \int_0^{\chi_G} \delta_m(\chi_L, \hat{\theta}) W_L(z_L, z_G) d\chi_L. \quad (1)$$

Here, $\hat{\theta}$ is the direction on the sky. $\delta_m(\chi_L, \hat{\theta})$ is the matter overdensity (lens) at direction $\hat{\theta}$ and comoving angular distance $\chi_L \equiv \chi(z_L)$ to redshift z_L . $\chi_G \equiv \chi(z_G)$ is the comoving angular diameter distance to the source. Both χ_L and χ_G are in unit of c/H_0 , where H_0 is the present day Hubble constant. The lensing kernel

$$W_L(z_L, z_G) = \frac{3}{2} \Omega_m (1 + z_L) \chi_L \left(1 - \frac{\chi_L}{\chi_G}\right). \quad (2)$$

when $z_L < z_G$ and is zero otherwise. Ω_m is the present day matter density in unit of the critical density. The lensing power spectrum is given by the following Limber equation,

$$C_{ij}^{GG}(\ell) = \frac{\pi}{\ell} \int_0^\infty \Delta_m^2(k = \frac{\ell}{\chi_L}, z_L) W_i(z_L) W_j(z_L) \chi_L d\chi_L. \quad (3)$$

Here, W_i is the lensing kernel W_L averaged over the i -th redshift bin, defined by Eq. A2.

For two-point statistics, weak lensing surveys thus provide three sets of correlations. Throughout this paper, we will work in the Fourier space (multipole ℓ space) and focus on the corresponding angular power spectra. The first one is the angular cross correlation power spectrum between galaxy ellipticity (κ^s) in the i -th redshift bin and the one in the j -th redshift bin, $C_{ij}^{(1)}(\ell)$.

$$C_{ij}^{(1)}(\ell) = C_{ij}^{GG}(\ell) + C_{ij}^{IG}(\ell) + C_{ji}^{IG}(\ell) + C_{ij}^{II}(\ell). \quad (4)$$

Here, $C_{ij}^{\alpha\beta}$ is the angular cross correlation power spectrum between quantity α in the i -th redshift bin and quantity β in the j -th redshift bin. $\alpha, \beta = G, I, g$, where the superscript (or subscript in denoting the redshift and distance) G denotes gravitational lensing (κ), I the galaxy intrinsic alignment (non-random intrinsic ellipticity) and g the galaxy number density distribution in the corresponding redshift bin (δ_Σ).

The ellipticity-ellipticity pair relevant to the current paper has $i < j$. Since $C_{ji}^{IG} \ll C_{ij}^{IG}$ as long as the catastrophic error is reasonably small, we have

$$C_{ij}^{(1)}(\ell) \simeq C_{ij}^{GG}(\ell) + C_{ij}^{IG}(\ell) + 2C_{ij}^{II}(\ell) \quad \text{when } i < j. \quad (5)$$

For bin size $\Delta z \gtrsim 0.2$, as long as the catastrophic photo-z errors are reasonably small, C_{ij}^{II} of non-adjacent bins ($i < j - 1$) is in general negligible with respect to the GI correlation (e.g. Schneider & Bridle 2009), because the II correlation only exists at small line-of-sight separation. However, for adjacent bins ($i = j - 1$), the II correlation can be non-negligible for $\Delta z \sim 0.2$ (Schneider & Bridle 2009). The self-calibration technique proposed in the current paper is not able to correct for the II correlation, for which other methods (Joachimi & Schneider 2008, 2009; Zhang 2010) may be applicable. It only applies to correct for the GI correlation C^{GI} . We express the GI correlation as a fractional error to the lensing measurement,

$$f_{ij}^I(\ell) \equiv \frac{C_{ij}^{IG}(\ell)}{C_{ij}^{GG}(\ell)}. \quad (6)$$

f_{ij}^I is the fractional GI contamination to the lensing measurement. f_{ij}^I ($i < j$) and f_{ik}^I ($i < k$) are not independent, since both describe the intrinsic alignment in the i -th redshift bin and thus

$$\frac{f_{ij}^I(\ell)}{f_{ik}^I(\ell)} \simeq \left(\frac{W_{ij}}{W_{ik}} \right) \left(\frac{C_{ik}^{GG}(\ell)}{C_{ij}^{GG}(\ell)} \right). \quad (7)$$

However, for its clear meaning as a fractional error in the lensing measurement, and for uncertainties in the intrinsic alignment modeling, we adopt it, instead of C_{ij}^{IG} itself, to express the GI contamination throughout the paper. The measured GI correlation is an anti-correlation ($f_{ij}^I < 0$), because the lensing induced shear is tangential to the gradient of the gravitational potential while the intrinsic shear is parallel to the gradient. Throughout the paper, we often neglect this negative sign, since we will work under the limit $f_{ij}^I \ll 1$ and thus its sign does not affect our error analysis. Our self-calibration technique works in principle for any value of f_{ij}^I . The results presented in this paper can be extended to other values of f_{ij}^I straightforwardly.

The second correlation is between the galaxy density (δ_Σ) in the i -th redshift bin and the galaxy ellipticity (κ^s) in the j -th redshift bin, $C_{ij}^{(2)}$. Galaxy-galaxy lensing in general focuses on $C_{ij}^{(2)}$ ($i < j$). Zhang et al. (2009) showed that the measurement $C_{ij}^{(2)}$ ($i > j$) contains valuable information on photo-z outliers. The one relevant for our GI self-calibration is

$$C_{ii}^{(2)}(\ell) = C_{ii}^{gG}(\ell) + C_{ii}^{gI}(\ell). \quad (8)$$

The C_{ii}^{gI} term contains here clearly contains valuable information on the intrinsic alignment. The two terms on the right hand side has different dependences on photo-z error. Larger photo-z errors tend to increase C^{gG} and decrease C^{gI} .

The third set of cross correlation is between galaxy density (δ_Σ) in the i -th redshift bin and j -th redshift bin, $C_{ij}^{(3)}$. It has been shown that $C_{ij}^{(3)}$ ($i \neq j$) is a sensitive probe of photo-z outliers (Schneider et al. 2006; Zhang et al. 2009). Our GI self-calibration requires the measurement

$$C_{ii}^{(3)}(\ell) = C_{ii}^{gg}(\ell). \quad (9)$$

Self-calibration of GI contamination

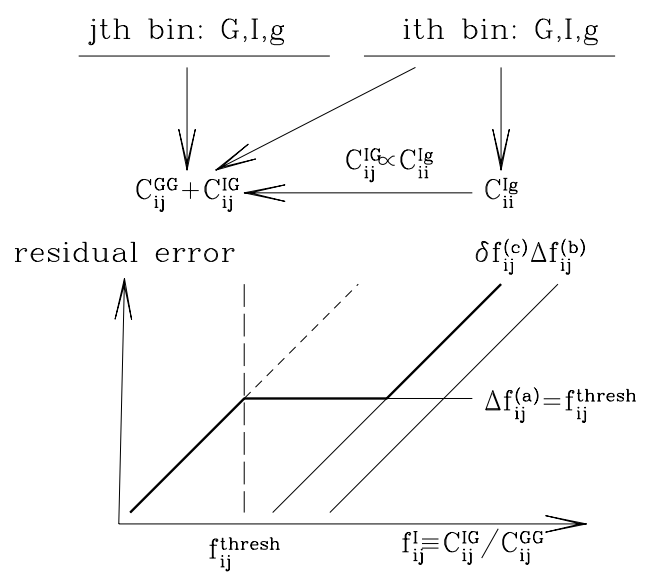


FIG. 1.— A schematic description of the GI self-calibration technique. Here, G denotes gravitational lensing, I the non-random galaxy intrinsic alignment and g the galaxy number density distribution in the corresponding redshift bin. Here, galaxies in the j -th redshift bin have higher photo- z than those in the i -th redshift bin. The GI contamination C_{ij}^{IG} is expressed as fractional error in lensing power spectrum C_{ij}^{GG} , namely, $f_{ij}^I \equiv C_{ij}^{IG}/C_{ij}^{GG}$. The self-calibration operates when f_{ij}^I is bigger than certain threshold f_{ij}^{thresh} . Depending on the fiducial value of f_{ij}^I , residual GI contamination from different sources dominates, which we highlight as bold lines in lower part of the figure. Refer to Eq. 6, 19, 21 & 24 for definitions of corresponding variables.

Our self-calibration aims to estimate and eliminate the GI contamination C_{ij}^{IG} in Eq. 5 from the measurements $C_{ii}^{(2)}$ (Eq. 8) and $C_{ii}^{(3)}$ (Eq. 9), both are available in the same survey. This method is thus dubbed the GI self-calibration.

For the self-calibration to work, $f_{ij}^I(\ell)$ must be sufficiently large for the band power $C_{ii}^{Ig}(\ell)$ at the corresponding ℓ bin to be detected through the measurement $C_{ii}^{(2)}(\ell)$. We denote the threshold as $f_{ij}^{\text{thresh}}(\ell)$. For brevity, we often neglect the argument ℓ in f_{ij} . When $f_{ij}^I \geq f_{ij}^{\text{thresh}}$, we can apply the self-calibration to reduce the GI contamination. The residual GI contamination after the self-calibration is expressed in as *residual fractional error* on the lensing measurement, in which Δf_{ij} denotes statistical error and δf_{ij} denotes systematical error. Thus the self-calibration performance is quantified by f_{ij}^{thresh} , Δf_{ij} and δf_{ij} . The smaller these quantities are, the better the performance. We will numerically evaluate these quantities later.

2.2. The self-calibration

The starting point of the GI self-calibration is a simple scaling relation between C_{ij}^{IG} and C_{ii}^{Ig} that we find,

$$C_{ij}^{IG}(\ell) \simeq \left[\frac{W_{ij}\Delta_i}{b_i(\ell)} \right] C_{ii}^{Ig}(\ell). \quad (10)$$

Here, $\chi_i \equiv \chi(\bar{z}_i)$, $b_i(\ell)$ is the galaxy bias in this redshift bin at the corresponding angular scale ℓ . W_{ij} is the weighted lensing kernel defined by

$$W_{ij} \equiv \int_0^\infty dz_L \int_0^\infty dz_G [W_L(z_L, z_G) \bar{n}_i(z_L) \bar{n}_j(z_G)] . \quad (11)$$

Notice that \bar{n}_i is normalized such that $\int_0^\infty \bar{n}_i(z) dz = 1$. Δ_i is an effective width of the i -th redshift bin, defined by

$$\Delta_i^{-1} \equiv \int_0^\infty \bar{n}_i^2(z) \frac{dz}{d\chi} dz . \quad (12)$$

Refer to the appendix §A for the derivation.

This scaling relation arises from the fact that, both GI and I-g cross correlations are determined by the matter-intrinsic alignment in the i -th redshift bin. The prefactors in Eq. 10 are simply the relative weighting between the two. In this sense, this scaling relation is rather generic.

The basic procedure of the self-calibration, as illustrated in Fig. 1, is as follows.

- Extract C_{ii}^{Ig} from the measurement $C_{ii}^{(2)}$ in the i -th photo- z bin. This exercise is non-trivial, since $C_{ii}^{(2)}$ actually measures the sum of C_{ii}^{Ig} and C_{ii}^{Gg} , and C_{ii}^{Gg} is often non-negligible due to relatively large photo- z error. We find a method to simultaneously measure the two without resorting to spect- z information. The idea will be elaborated in §2.3 and the measurement error in C_{ii}^{Ig} will be calculated in §3.1.
- Measure the galaxy bias $b_i(\ell)$ from the measurement $C_{ii}^{(3)}(\ell)$ (§3.2).
- Calculate C_{ij}^{IG} from the above measurements and Eq. 10 and then subtract it from Eq. 4.

2.3. Measuring C_{ii}^{Ig}

An obstacle in measuring C_{ii}^{Ig} comes from the contamination C_{ii}^{Gg} (Eq. 8). For spectroscopic sample, this contamination is straightforward to eliminate. We just throw away pairs where the redshift of the galaxy to measure the shape is lower than the one to measure the number density (Mandelbaum et al. 2006; Hirata et al. 2007; Okumura & Jing 2009). This method is robust, however limited to the spec- z sample.

For photo- z sample, the above technique does not work, since the photo- z error is large. For it, the true galaxy distribution, even for photo- z bin size $\Delta z \rightarrow 0$, has relatively large width $\geq \sim 0.1(1+z)$, no matter how narrow the photo- z bin is. In practice, the photo- z bin size is often $\gtrsim 0.2$, which further increases the effective width. Thus, a galaxy in this photometric redshift bin has large chance to lens another galaxy in the same redshift bin, with a non-negligible lensing weight. For this reason, C_{ii}^{Gg} may not be negligible comparing to C_{ii}^{Ig} , even if the photo- z bin size is infinitesimal. We have numerically compared C_{ii}^{Gg} with C_{ii}^{Ig} calculated based on the intrinsic alignment model of Schneider & Bridle (2009) along their fiducial parameters, and found that

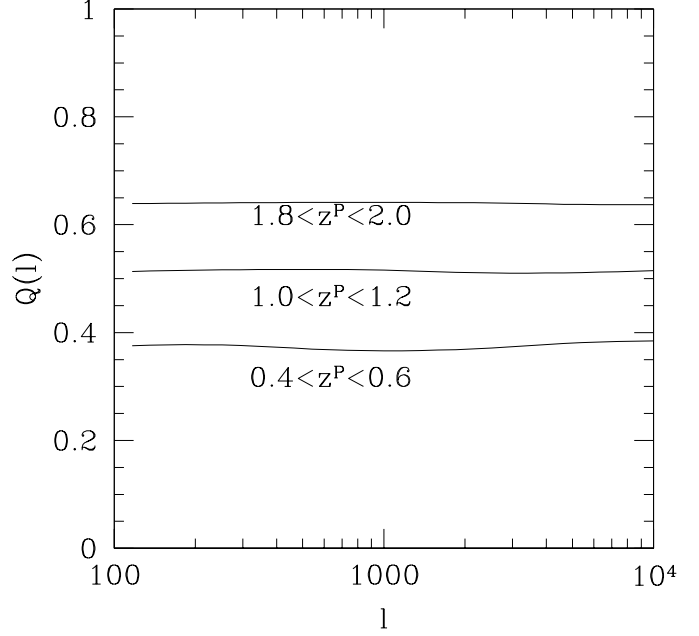


FIG. 2.— $Q_i(\ell) \equiv C_{ii}^{Gg}(\ell)/C_{ii}^{Ig}(\ell)$ describes the suppression of the galaxy-galaxy correlation in the same redshift bin after throwing away those pairs with source redshift (photo- z) higher than lens redshift (photo- z). Only when Q deviates significantly from unity, can we extract the I-g correlation from the shape-density correlation measurement in the same redshift bin. Q is nearly scale independent, since it is the ratio of two power spectra of similar shape. Overall, $Q \sim 1/2$. It increases with redshift, as expected from larger photo- z rms error at higher redshift and hence larger effective redshift width. This figure is a key result to demonstrate the feasibility of the self-calibration technique.

the two terms can indeed be comparable. For example, at a typical lensing angular scale $\ell = 10^3$ and a typical redshift $z = 1$, C_{ii}^{Gg}/C_{ii}^{Ig} is 30% for vanishing bin size and increases with bin size. Only when the redshift is sufficiently low or the redshift error and the bin size are both sufficiently small, may the G-g correlation be safely neglected.

Nevertheless, the photo- z measurement contains useful information and allows us to measure C_{ii}^{Ig} . Our method to separate C_{ii}^{Gg} from C_{ii}^{Ig} relies on their distinctive and predictable dependences on the relative position of galaxy pair. Let's denote the redshift of one galaxy in the pair for the shape measurement as z_G^P and the other one for the number density measurement as z_g^P . The I-g correlation does not depend on the ordering along the line-of-sight, as long as the physical separation is fixed. In another word, the I-g correlation for the pair with $z_G^P > z_g^P$ is statistically identical to the pair with $z_G^P < z_g^P$, as long as $|z_G^P - z_g^P|$ fixes. On the other hand, the G-g correlation cares about the ordering along the line-of-sight. The G-g correlation for the pair with $z_G^P > z_g^P$ is statistically larger than the pair with $z_G^P < z_g^P$, due to the lensing geometry dependence.

We can then construct two observables on the ellipticity-density correlation. (1) One is $C_{ii}^{(2)}(\ell)$, weighting all pairs equally. (2) The other is $C_{ii}^{(2)}|_S(\ell)$, in which we only count the cross correlation between those pairs

with $z_G^P < z_g^P$. The subscript “S” denotes the corresponding quantities under this weighting. From the argument above, we have $C_{ii}^{Ig}(\ell) = C_{ii}^{Ig}|_S(\ell)$. On the other hand, $C_{ii}^{Gg}|_S(\ell) < C_{ii}^{Gg}(\ell)$, since those $z_G^P > z_g^P$ pairs that we disregard contribute more to the lensing-galaxy correlation. We denote the suppression by

$$Q(\ell) \equiv \frac{C_{ii}^{Gg}(\ell)|_S}{C_{ii}^{Gg}(\ell)}. \quad (13)$$

Q is sensitive to photo- z errors. In general catastrophic errors drive Q towards 1. $Q = 1$ if the photo- z is completely wrong and has no correlation with the true redshift and $Q = 0$ if the photo- z is 100% accurate. Usually $0 < Q < 1$. Q can be calculated from the galaxy redshift distribution (the appendix §B) and is thus in principle an observable too. From the two observables

$$\begin{aligned} C_{ii}^{(2)}(\ell) &= C_{ii}^{Ig}(\ell) + C_{ii}^{Gg}(\ell), \\ C_{ii}^{(2)}|_S(\ell) &= C_{ii}^{Ig}(\ell) + C_{ii}^{Gg}|_S(\ell), \end{aligned} \quad (14)$$

We obtain the solution to C_{ii}^{Ig} ,

$$\hat{C}_{ii}^{Ig}(\ell) = \frac{C_{ii}^{(2)}|_S(\ell) - Q(\ell)C_{ii}^{(2)}(\ell)}{1 - Q(\ell)}. \quad (15)$$

For it to be non-singular, Q must deviate from unity ($Q < 1$). We numerically evaluate this quantity and find that, for the survey specifications presented in this paper, $Q \sim 1/2$ (Fig. 2). The significant deviation of Q from unity is not a coincidence. It is in fact a manifestation that the lensing efficiency changes significantly across the redshift interval σ_P . We thus expect the C_{ii}^{Ig} estimator (Eq. 15) to be applicable in general.

3. ERROR ESTIMATION

Unless explicitly specified, we will target at LSST throughout this paper to estimate the performance of the self-calibration technique proposed above. LSST plans to cover half the sky ($f_{\text{sky}} = 0.5$) and reach the survey depth of ~ 40 galaxies per arcmin². We adopt the galaxy number density distribution as $n(z) \propto z^2 \exp(-z/0.5)$, the rms shape error $\gamma_{\text{rms}} = 0.18 + 0.042z$ and photo- z scatter $\sigma_P = 0.05(1 + z)$. We split galaxies into photometric redshift bins with $\Delta z_i = 0.2$ centered at $\bar{z}_i = 0.2(i + 1)$ ($i = 1, 2, \dots$).²

3.1. Measurement error in C_{ii}^{Ig}

Both $C_{ii}^{(2)}$ and $C_{ii}^{(2)}|_S$ have cosmic variance and shot noise errors, which propagate into C_{ii}^{Ig} extracted from the estimator Eq. 15. The error estimation on C_{ii}^{Ig} is non-trivial since errors in $C_{ii}^{(2)}$ and $C_{ii}^{(2)}|_S$ are neither

² The choice of redshift bin is somewhat arbitrary. For example, we can include a lower redshift bin with $\bar{z}_i = 0.2$ ($0.1 < z^P < 0.3$). The self-calibration certainly works for this bin, since the I-g cross correlation in this bin is easier to extract due to weaker lensing signal and hence weaker G-g in this bin. The major reason that we do not include this bin is that the lensing signal in this bin is weak. Weak lensing signal may cause confusion on the performance of the self-calibration, due to our choice to express the GI correlation before and after the self-calibration as ratios with respect to the lensing signal. For example, Fig. 3 shows that Δf_{ij} increases toward low redshifts. But it is an manifestation of weak lensing signal instead of poor performance of the self-calibration.

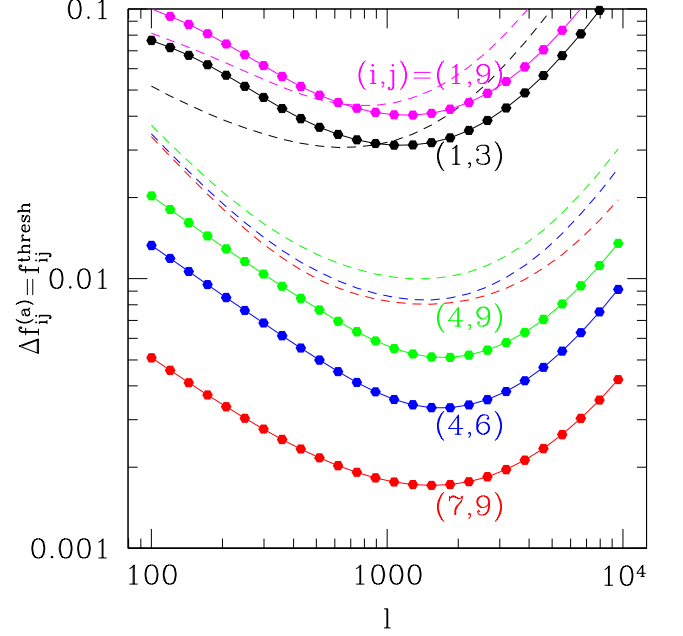


FIG. 3.— The threshold of the applicability of the self-calibration technique f_{ij}^{thresh} and the residual statistical uncertainty $\Delta f_{ij}^{(a)}$ (solid lines with data points). Refer to Eq. 19 for the definition of $\Delta f_{ij}^{(a)}$. The self-calibration applies for sufficiently large GI contamination ($f_{ij}^I > f_{ij}^{\text{thresh}}$) and reduces the fractional error from f_{ij}^I to $\Delta f_{ij}^{(a)}$. Here, the superscript (a) denotes the error from the C_{ii}^{Ig} measurement. Notice that $f_{ij}^{\text{thresh}} = \Delta f_{ij}^{(a)}$ and both are insensitive to the fiducial f_{ij}^I . The cosmic variance in the lensing field and the random shape fluctuation sets the minimum fractional statistical error e_{ij}^{min} in C_{ii}^{Gg} measurement, which we plot as dash lines. The numerical estimation shown is for redshift bins $\bar{z}_i = 0.2(i + 1)$ ($i = 1, 2, \dots$) and multipole bin size $\Delta \ell = 0.2\ell$ in LSST. In general $\Delta f_{ij}^{(a)} < e_{ij}^{\text{min}}$ and thus the residual error after the self-calibration is negligible. Since both $\Delta f_{ij}^{(a)}$ and e_{ij}^{min} scale in similar ways, this conclusion holds in general for other lensing surveys.

completely uncorrelated, nor completely correlated. The derivation is lengthy, so we leave it in the appendix §C. The final result of the rms error ΔC_{ii}^{Ig} in a bin with width $\Delta \ell$ is

$$\begin{aligned} (\Delta C_{ii}^{Ig})^2 &= \frac{1}{2\ell \Delta \ell f_{\text{sky}}} \left(C_{ii}^{gg} C_{ii}^{GG} + \left[1 + \frac{1}{3(1-Q)^2} \right] \right. \\ &\quad \times \left[C_{ii}^{gg} C_{ii}^{GG,N} + C_{ii}^{gg,N} (C_{ii}^{GG} + C_{ii}^{II}) \right] \\ &\quad \left. + C_{ii}^{gg,N} C_{ii}^{GG,N} \left[1 + \frac{1}{(1-Q)^2} \right] \right). \end{aligned} \quad (16)$$

Here, the superscript “N” denotes measurement noise such as shot noise in galaxy distribution and random shape noise. $C_{ii}^{gg,N} = 4\pi f_{\text{sky}}/N_i$ and $C_{ii}^{GG,N} = 4\pi f_{\text{sky}} \gamma_{\text{rms}}^2/N_i$, where N_i is the total number of galaxies in the i -th redshift bin.

From Eq. 16, ΔC_{ii}^{Ig} is insensitive to the intrinsic alignment, as long as the II correlation is sub-dominant with respect to the GG correlation. We will work at this limit. If the intrinsic alignment is too small, the measurement error ΔC_{ii}^{Ig} will be larger than C_{ii}^{Ig} . $\Delta C_{ii}^{Ig} = C_{ii}^{Ig}$ hence

sets a threshold f_{ij}^I . Combining Eq. 10 and the definition $f_{ij}^I \equiv C_{ij}^{IG}/C_{ij}^{GG}$ (Eq. 6), we obtain this threshold as

$$f_{ij}^{\text{thresh}} = \left(\frac{\Delta C_{ii}^{Ig}}{C_{ij}^{GG}} \right) \left(\frac{W_{ij} \Delta_i}{b_i(\ell)} \right). \quad (17)$$

f_{ij}^{thresh} has two important meanings. (1) It describes the minimum intrinsic alignment ($f_{ij}^I = f_{ij}^{\text{thresh}}$) that can be detected through our method with $S/N=1$. Thus it also defines the lower limit beyond which our self-calibration technique is no longer applicable. (2) It describes the self-calibration accuracy resulting from C_{ii}^{Ig} measurement error. The measurement error ΔC_{ii}^{Ig} propagates into an error in C_{ij}^{IG} determination through Eq. 10 and hence leaves a residual statistical error in the GG measurement. We denote this error as $\Delta f_{ij}^{(a)}$. Since $\Delta f_{ij}^{(a)}/f_{ij}^I = \Delta C_{ii}^{Ig}/C_{ii}^{Ig}$, combining Eq. 10, we have

$$\Delta f_{ij}^{(a)} = \left(\frac{\Delta C_{ii}^{Ig}}{C_{ii}^{GG}} \right) \left(\frac{W_{ij} \Delta_i}{b_i(\ell)} \right). \quad (18)$$

Also, we find an important relation between the two,

$$\Delta f_{ij}^{(a)} = f_{ij}^{\text{thresh}}. \quad (19)$$

This relation can be understood in this way. When the intrinsic alignment $f_{ij}^I > f_{ij}^{\text{thresh}}$, it can be inferred through measurement in C_{ii}^{Ig} and hence be corrected. Since measurement C_{ii}^{Ig} has statistical error ΔC_{ii}^{Ig} (Eq. 16), this correction is imperfect. The residual error in f_{ij}^I is set by the same ΔC_{ii}^{Ig} determining f_{ij}^{thresh} , so we have the relation Eq. 19. If only our method is applied, we are only able to detect the intrinsic alignment with an amplitude $f_{ij}^I > f_{ij}^{\text{thresh}}$ and correct it to a level of $\Delta f_{ij}^{(a)} = f_{ij}^{\text{thresh}}$.

Once the intrinsic alignment is sufficiently large to be detected ($f_{ij}^I > f_{ij}^{\text{thresh}}$), our self-calibration technique can detect and thus eliminate the GI contamination. It renders a systematical error in lensing measurement with amplitude f_{ij}^I into a statistical error with rms $\Delta f_{ij}^{(a)} = f_{ij}^{\text{thresh}} < f_{ij}^I$. We notice that $\Delta f_{ij}^{(a)}$ is insensitive to f_{ij}^I .

Numerical results on $\Delta f_{ij}^{(a)} = f_{ij}^{\text{thresh}}$ are evaluated through Eq. 18 along with Eq. 16 and are shown in Fig. 3. For comparison, we also plot the *minimum G-G error* in the C_{ij}^{GG} measurement. It is the rms fluctuation induced by the cosmic variance in the G-G correlation and shot noise due to random galaxy ellipticities, in idealized case of no other error sources such as the intrinsic alignment. This minimum G-G error sets the ultimate lower limit of the fractional measurement error on C_{ij}^{GG} ($i \neq j$),

$$(e_{ij}^{\min})^2 = \frac{C_{ij}^{GG,2} + (C_{ii}^{GG} + C_{ii}^{GG,N})(C_{jj}^{GG} + C_{jj}^{GG,N})}{2\ell\Delta\ell f_{\text{sky}} C_{ij}^{GG,2}}. \quad (20)$$

When $\Delta f_{ij}^{(a)}$ is smaller than e_{ij}^{\min} , the residual error after the self-calibration will then be negligible, meaning a self-calibration with little cosmological information loss. We

find that this is indeed the case in general. Fig. 3 is the forecast for LSST.³ Since both $\Delta f_{ij}^{(a)}$ and e_{ij}^{\min} scale in a similar way with respect to survey specifications such as the sky coverage and galaxy number density, this conclusion also holds for other lensing surveys such as CFHTLS, DES, Pan-Starrs, Euclid and JDEM.

How can the GI contamination be corrected to an accuracy even below the statistical limit of GG measurement? Equivalently, why is f_{ij}^I as small as the one shown in Fig. 3 detectable? This surprising result requires some explanation. The reason is that C_{ii}^{Ig} is amplified with respect to C_{ij}^{IG} by a large factor $1/W_{ij}\Delta_i \sim O(10^2)$ (Eq. 10). Thus a small GI contamination ($f_{ij}^I \ll 1$) can still cause a detectable C_{ii}^{Ig} . This explains the small $f_{ij}^{\text{thresh}} = \Delta f_{ij}^{(a)}$.

3.2. Measuring the galaxy bias

The second uncertainty in the self-calibration comes from the measurement of the galaxy bias, $\Delta b_i(\ell)$. From Eq. 10, this uncertainty induces a residual statistical error

$$\Delta f_{ij}^{(b)} = f_{ij}^I (\Delta b_i(\ell)/b_i(\ell)). \quad (21)$$

There are several possible ways to obtain b_ℓ such as combining galaxy-galaxy lensing and galaxy clustering measurements (e.g. Sheldon et al. 2004), combining 2-point and 3-point galaxy clustering (e.g. (Guo & Jing 2009)), fitting against the halo occupation (Zheng et al. 2005) and conditional luminosity function (Yang et al. 2003), or analyzing the counts-in-cells measurements (Szapudi & Pan 2004). Alternatively, $b_i(\ell)$ can be inferred from the galaxy density-galaxy density correlation measurement alone, $C_{ii}^{(3)}(\ell) = C_{ii}^{gg}(\ell) \simeq b_\ell^2 C_{ii}^{mm}(\ell)$. Here, C_{ii}^{mm} is the matter angular power spectrum, with the same weighting as galaxies. Both uncertainties in the theoretical prediction of C_{ii}^{mm} and measurement error in $C_{ii}^{(3)}$ affects the $b_i(\ell)$ measurement. Given a cosmology, one can evolve the matter power spectrum tightly constrained at the recombination epoch by CMB experiment to low redshift and thus predict C_{ii}^{mm} . As long as the associated uncertainty is smaller than 10%, the induced error will be sub-dominant to the systematical error discussed later in §3.3. This is an important issue for further investigation.

On the other hand, the statistical error in $b_i(\ell)$ induced by the galaxy clustering measurement error is

$$\frac{\Delta b_i(\ell)}{b_i(\ell)} \sim \frac{1}{2} \sqrt{\frac{1}{\ell\Delta\ell f_{\text{sky}}}} \times \left(1 + \frac{C_{ii}^{gg,N}(\ell)}{C_{ii}^{gg}(\ell)} \right). \quad (22)$$

This rough estimation suffices for the purpose of this paper, for which the reason will be clear latter soon. This error is negligible for a number of reasons. (1) It is in general much smaller than the systematical error in the scaling relation, $\delta f_{ij}^{(c)}$. As will be shown in §3.3, $\delta f_{ij}^{(c)} \sim 0.1 f_{ij}^I$. On other other hand, $b_i(\ell)$ can in general be measured with better than 10% accuracy.

³ We do notice that in some cases especially when one of the photo bin is at low redshift, $\Delta f_{ij}^{(a)} > e_{ij}^{\min}$ (Fig. 3), leading to non-negligible loss in cosmological information for relevant redshift bins.

For example, for LSST at $\ell = 100$ with $\Delta\ell = 0.2\ell$, $\Delta b_i(\ell)/b_i(\ell) \simeq 1.6\%$. $b_i(\ell)$ can be measured with higher accuracy toward smaller scales, until shot noise dominates. Thus $\Delta f_{ij}^{(b)} \ll \delta f_{ij}^{(c)}$ at relevant scales. (2) It is smaller than the minimum statistical error in C_{ij}^{GG} measurement (Fig. 3). First of all, galaxy clustering measurement is in general more accurate than lensing measurement. Second, the impact of uncertainty in $b_i(\ell)$ on the self-calibration is modulated by a factor f_{ij}^I ($\Delta f_{ij}^{(b)} = f_{ij}^I(\Delta b_i(\ell)/b_i(\ell))$). Unless $f_{ij}^I > 1$, $\Delta f_{ij}^{(b)}$ is suppressed. Thus we expect that the $b_i(\ell)$ induced error $\Delta f_{ij}^{(b)}$ is negligible even to the minimum statistical error in C_{ij}^{GG} measurement. From the above general argument, this conclusion should hold for most, if not all, lensing surveys. We show one example of LSST. Even for a rather large $f_{ij}^I = 1$, uncertainty in $b_i(\ell)$ only causes a statistical error of $\Delta f_{ij}^{(b)} = 1.6\%$ at $\ell = 100$, negligible comparing to statistical uncertainties in C_{ij}^{GG} measurement (Fig. 3). The above conclusions are safe even if Eq. 22 underestimates the error in $b_i(\ell)$ by a factor of a few. This is the reason that we do not seek a more robust estimation on the measurement error in $b_i(\ell)$.

From the above argument, the errors $\Delta f_{ij}^{(b)}$ and $\Delta f_{ij}^{(a)}$ arise from different sources and thus are independent to each other. The combined error is then $\sqrt{(\Delta f_{ij}^{(a)})^2 + (\Delta f_{ij}^{(b)})^2}$. Since the galaxy bias induced error is likely sub-dominant to either the error source (a) or to the one will be discussed in §3.3, we will neglect it for the rest of the paper.

3.3. The accuracy of the C_{ii}^{IG} - C_{ii}^{Ig} relation

A key ingredient in the self-calibration is Eq. 10, which links the observable C_{ii}^{Ig} to the GI contamination. However, Eq. 10 is not exact and we quantify its accuracy by

$$\epsilon_{ij}(\ell) \equiv \frac{b_i(\ell)C_{ij}^{IG}(\ell)}{W_{ij}\Delta_i C_{ii}^{Ig}(\ell)} - 1. \quad (23)$$

ϵ_{ij} also quantifies the induced residual systematic error,

$$\delta f_{ij}^{(c)} = \epsilon_{ij} f_{ij}^I. \quad (24)$$

We present a rough estimation by adopting a toy model

$$\Delta_{mI}^2(k, z) \propto \Delta_{gI}^2(k, z) \propto \Delta_m^2(k, z)(1+z)^\beta \quad (25)$$

with $\beta = -1, 0, 1$. Here, Δ_{mI}^2 , Δ_{gI}^2 and Δ_m^2 are the 3D matter-intrinsic alignment, galaxy-intrinsic alignment cross correlation power spectrum (variance) and matter power spectrum, respectively. The accuracy of Eq. 10 is not only affected by the scale dependence of corresponding 3D power spectra, but also their redshift evolution (the appendix A). Theoretical models of the intrinsic alignment (e.g. Schneider & Bridle 2009) show that the redshift evolution may not follow the evolution in the density field. For this reason, we add an extra redshift dependence $(1+z)^\beta$ in Eq. 25. This recipe is completely arbitrary, but it helps to demonstrate the robustness of Eq. 10.

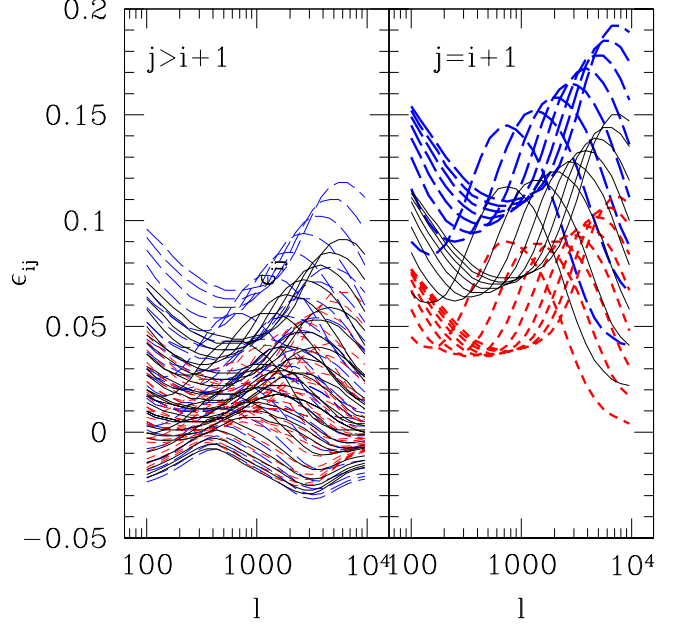


FIG. 4.— ϵ_{ij} quantifies the accuracy of Eq. 10, which links the observable C_{ii}^{Ig} to the GI contamination C_{ij}^{IG} . It thus quantifies a dominant systematical error of the self-calibration technique, $\delta f_{ij}^{(c)} = \epsilon_{ij} f_{ij}^I$. Solid, dotted and dash lines represent three toy models of the intrinsic ellipticity evolution. Usually, Eq. 10 is accurate within 10%. However, for those adjacent bins with $i, j = i+1$, due to stronger redshift dependence of the lensing kernel, Eq. 10 is least accurate and ϵ_{ij} is largest (right panel).

Numerical results are shown in Fig. 4. We see that for most ij pairs, $|\epsilon_{ij}|$ is less than 10%, meaning that we are able to suppress the GI contamination by a factor of 10 or larger, if other errors are negligible.

We notice that the largest inaccuracy of Eq. 10 occurs for those adjacent bins ($i, j = i+1$), which is 10%-20%. This is caused by the lensing geometry dependence. Eq. 10 would be quite accurate if the integrand in Eq. A1 & A3 varies slowly with redshift. However, since the i -th bin and the $j = i+1$ -th bin are close in redshift, the lensing kernel $W_j(z)$ varies quickly over the i th redshift bin. This fast redshift evolution degrades the accuracy of the scaling relation and thus causes a larger $|\epsilon_{ij}|$. On the other hand, $W_j(z)$ changes more slowly over other bins with $i \neq j-1$, since now the source-lens separation is larger. For this reason, Eq. 10 is more accurate for these bins. The self-calibration technique does not work excellently for adjacent bins, but a factor of 5 reduction in the GI contamination is still achievable.

The scaling relation accuracy is sensitive to the photo- z accuracy, $\epsilon_{ij} \propto \sigma^2 \simeq \sigma_p^2 + (\Delta z)^2/12$. Here, σ is the rms redshift dispersion in the corresponding redshift bin. One can obtain the above relation by perturbing Eq. A1 & A3 around the median redshift and keeping up to the second order. Thus, if photo- z accuracy can be significantly improved, the accuracy of Eq. 10 can be significantly improved too. For example, if $\sigma_p = 0.03(1+z)$ instead of the fiducial value $0.05(1+z)$, the scaling relation accuracy can be improved by a factor of ~ 2 -3. This would allow us to suppress the GI contamination by a factor of

10-20 or even higher. The shape of the photo-z PDF also matters. Depending on which direction it is skewed, the scaling relation accuracy may be improved or degraded. In §4.2, we will discuss the impact of catastrophic error, which presents as significant deviation from the adopted Gaussian PDF.

The accuracy of the scaling relation may also be improved by better modeling. ϵ_{ij} has (much) larger chance to be positive (Fig. 4). This behavior is likely general, not limited to the intrinsic ellipticity toy models we investigate. In deriving the scaling relation, both C_{ii}^{Ig} and C_{ij}^{IG} are evaluated at the middle redshift \bar{z}_i . The weighting function in C_{ii}^{Ig} roughly peaks at \bar{z}_i while the one in C_{ij}^{IG} peaks at lower redshift, due to the monotonous decreasing of $W_j(z)$ with redshift (until it vanishes). It is this imbalance causing the general behavior $\epsilon_{ij} > 0$. It also shed light on improving C_{ij}^{IG} - C_{ii}^{Ig} relation and reducing the associated systematical error: an interesting project for future investigation.

3.4. General behavior of the residual errors

Depending on the nature of the GI correlation, either the error in C_{ii}^{Ig} measurement or the error in the scaling relation can dominate the error budget of the self-calibration, while the one from the galaxy bias is likely sub-dominant. Fig. 1 demonstrates the relative behavior of the three error sources in the self-calibration. The bold lines highlight the dominant error, as a function of the intrinsic alignment amplitude f_{ij}^I . There are several regimes.

- $f_{ij}^I \leq f_{ij}^{\text{thresh}}$. The intrinsic alignment is too weak to be detected in the galaxy-lensing correlation. For this reason, the self-calibration technique is not applicable. However, this usually also mean the intrinsic alignment is negligible in lensing-lensing measurement, comparing to the associated minimum statistical error (Fig. 3). Thus there is no need to correct for the GI contamination in this case. However, there are important exceptions to the above conclusion. For example, from Fig. 3, when one photo-z bin is at sufficiently low redshift, the GI contamination is undetectable by our method, but the systematical error it induces is non-negligible. Furthermore, our method is insensitive to the intrinsic alignment which is weakly correlated to the density field. Such intrinsic alignment can cause large contamination to the lensing power spectrum C_{ii}^{GG} , but leaves no detectable feature in the ellipticity-density measurement $C_{ii}^{(2)}$. In these cases, other methods (e.g. Joachimi & Schneider 2008, 2009; Zhang 2010) shall be applied to correct for the intrinsic alignment.
- $f_{ij}^I > f_{ij}^{\text{thresh}}$. The self-calibration begins to work.
 - (1) $f_{ij}^I < \Delta f_{ij}^{\text{thresh}}/\epsilon_{ij}$. The statistical error induced by I-g measurement uncertainty dominates. However, this residual error, $\Delta f_{ij}^{(a)} = \Delta f_{ij}^{\text{thresh}}$, is usually negligible, comparing to the minimum statistical error e_{ij}^{min} in shear measurement ($\Delta f_{ij}^{(a)} <$

e_{ij}^{min} , Fig. 3). In this domain, the self-calibration technique is promising to work down to the statistical limit of lensing surveys.

- (2) $f_{ij}^I > \Delta f_{ij}^{\text{thresh}}/\epsilon_{ij}$. The systematical error arising from the imperfect scaling relation dominates. The fractional residual error in lensing-lensing measurement is $\delta f_{ij}^{(c)} = \epsilon_{ij} f_{ij}^I \sim 0.1 f_{ij}^I$. This error will be still sub-dominant to the lensing statistical fluctuation, if $f_{ij}^I < e_{ij}^{\text{min}}/\epsilon_{ij}$. If not the case, the self-calibration can work to suppress the GI contamination by a factor of 10. Other complementary techniques such as the nulling technique proposed by Joachimi & Schneider (2008, 2009) shall be applied to further reduce the residual GI contamination down to its statistical limit.

4. OTHER SOURCES OF ERROR

There are other sources of error, beyond the three ones discussed above. We discuss qualitatively on magnification bias, catastrophic photo-z error, stochastic galaxy bias and cosmological uncertainties. Based on simplified estimations, we conclude that none of them can completely invalidate the self-calibration technique. Quantitative and comprehensive evaluation of all these errors, including the ones in previous section, will be postpone elsewhere.

4.1. Magnification bias

Gravitational lensing not only distorts the shape of galaxies, but also alter their spatial distribution and induces magnification bias, or cosmic magnification (e.g. Scranton et al. (2005) and references therein). It changes the observed galaxy overdensity to $\delta_g^L = \delta_g + g(F)\kappa$. The function $g(F) = 2(-d \ln N(> F)/d \ln F - 1)$ is determined by the logarithmic slope of the (unlensed) galaxy luminosity function $N(> F)$ and is in principle measurable.

The magnification bias affects both $C_{ij}^{(1)}$, through a subtle source-lens coupling (Hamana 2001), and $C_{ij}^{(3)}$. However, these impacts are negligible, in the context of this paper. The magnification bias has a relatively larger effect on $C_{ii}^{(2)}$ and modifies Eq. 8 to

$$\begin{aligned} C_{ii}^{(2)} &= C_{ii}^{gG} + C_{ii}^{gI} + g_i(C_{ii}^{GG} + C_{ii}^{GI}) \\ &= [C_{ii}^{gG} + g_i C_{ii}^{IG}] + [C_{ii}^{gI} + g_i C_{ii}^{GG}]. \end{aligned} \quad (26)$$

Here g_i is the averaged $g(F)$ over galaxies in the i -th redshift bin, $g_i = \langle g_i(F) \rangle$. $g(F)$ is of order unity (e.g. Scranton et al. 2005). However, since it changes sign from bright end of the luminosity function to the faint end, We expect that the averaged g_i to be smaller than 1 for sufficiently deep surveys, $g_i < 1$.

Our goal is to measure C_{ii}^{gI} , with new contaminations from the magnification bias. We can apply the same weighting of the estimator Eq. 15 here. On one hand, both C_{ii}^{gI} and C_{ii}^{GG} are unchanged by this weighting. On the other hand, both C_{ii}^{GI} and C_{ii}^{gG} are reduced by virtually the same $1 - Q$. These behaviors mean that, the estimator Eq. 15 eliminates the combination $C_{ii}^{gG} + g_i C_{ii}^{IG}$ and measures the combination $C_{ii}^{gI} + g_i C_{ii}^{GG}$ in which the term $g_i C_{ii}^{GG}$ contaminates the I-g measurement.

$g_i C_{ii}^{GG}$ can not be eliminated completely, due to various sources of error. An obvious one is the measurement error in $g(F)$. At bright end, the galaxy number density drops exponentially and lensing modifies $N(> F)$ significantly for its steep slope. At faint end, the flux measurement noise is large. Catastrophic photo- z error is also an issue (Schneider et al. 2000). We will not estimate these errors for realistic surveys. Instead, we ask how stringent the requirement on the g_i and C_{ii}^{GG} measurements should be in order to make the impact of the magnification bias negligible.

Suppose the g_i measurement has an error δg_i and the C_{ii}^{GG} measurement has an error δC_{ii}^{GG} , the induced fractional error in C_{ij}^{GG} measurement is

$$\begin{aligned} & \frac{W_{ij} \Delta_i}{b_i} \frac{\delta g_i C_{ii}^{GG} + g_i \delta C_{ii}^{GG}}{C_{ij}^{GG}} \\ & < \frac{W_{ij} \Delta_i}{b_i} \left(|\delta g_i| + \left| g_i \frac{\delta C_{ii}^{GG}}{C_{ii}^{GG}} \right| \right) \\ & = O(10^{-3}) \left(\left| \frac{\delta g_i}{0.1} \right| + \left| \frac{g_i \delta C_{ii}^{GG} / C_{ii}^{GG}}{10\%} \right| \right). \end{aligned}$$

The above relation holds since $C_{ii}^{GG} < C_{ij}^{GG}$ ($i < j$), $b_i = O(1)$ and $W_{ij} \Delta_i = O(10^{-2})$. (1) If g_i itself is small ($|g_i| \lesssim 0.1$), then there is no need to correct for the $g_i C_{ii}^{GG}$ term since its influence is at the level of 0.1% and thus negligible. (2) If g_i is large, but it can be measured with an accuracy ± 0.1 , and if C_{ii}^{GG} can be measured with 10% accuracy, the magnification bias induced error will be $O(10^{-3})$. It can thus be safely neglected, comparing to the minimum statistical error in C_{ii}^{GG} (Fig. 3) or to other residual errors of the self-calibration technique (Fig. 3 & 4). Direct measurement of g_i from the observed (lensed) flux galaxy distribution in the redshift bin and the approximation $C_{ii}^{(1)} \simeq C_{ii}^{GG}$ likely meet the requirement, unless the II contamination is larger than 10%. (3) If the II contamination is larger than 10% and the measurement of C_{ii}^{GG} is heavily polluted, a more complicated method may work. We can split galaxies into flux bins and perform the above analysis to each flux bin. Since $g(F)$ changes in a known way across these flux bins, we are in principle able to eliminate the $g_i C_{ii}^{GG}$ term, combining all these measurements. For example, one can find an appropriate weighting function $W(F)$ such that $\langle g(F)W(F) \rangle = 0$. Although this method requires more accurate $g(F)$ measurement, it does not require measurement on C_{ii}^{GG} and thus avoids the II contamination and other associated errors.

Based on the above arguments, we expect that our self-calibration technique is safe against the magnification bias, although extra care is indeed required.

4.2. Catastrophic photo- z error

Numerical calculations we perform in this paper only consider a Gaussian photo- z PDF. Observationally, the photo- z PDF is more complicated, with non-negligible outliers (e.g. Jouvel et al. 2009; Bernstein & Huterer 2009). The existence of this catastrophic error affects the self-calibration technique through two ways. (1) It affects the accuracy of the Q estimation. (2) It affects the scaling relation Eq. 10. As shown in the appendix §A and further discussed in §3.3, a key condition in deriving Eq. 10 is that the true galaxy distribution in a

given photo- z bin is sufficiently narrow and smooth. So likely catastrophic error leads to degradation of the scaling relation (Eq. 10).⁴

From the appendix B, catastrophic error introduces bias to Q , mainly through its impact on η . Stage IV lensing projects need to control the outlier rate f_{cat} to $\sim 0.1\%$ accuracy (Hearin et al. 2010) in order for the induced systematical errors to be sub-dominant. If it is the case, we are able to perturb the photo- z PDF $p(z|z^P)$ in Eq. B5. We choose $|z - z^P| > \Delta$ as the criteria of the catastrophic error and then have $f_{\text{cat}} = \int_0^{z^P - \Delta} p(z|z^P) dz + \int_{z^P + \Delta}^\infty p(z|z^P) dz$. Since $f_{\text{cat}} \ll 1$, from Eq. B5, we find that the induced bias $\delta Q = O(f_{\text{cat}})$. As long as the goal $|f_{\text{cat}}| \lesssim 0.1\%$ can be achieved, the induced error in Q is less than 1% and hence not a significant source of error in the self-calibration. Furthermore, we are able to infer the statistically averaged photo- z PDF through self- and cross-calibrations of photo- z errors, even with the presence of large catastrophic errors (e.g. Schneider et al. 2006; Newman 2008; Zhang et al. 2009; Benjamin et al. 2010). Since Q can be predicted given the photo- z PDF, we are able to reduce the possible bias in Q , even if the actual $f_{\text{cat}} \gtrsim 0.1\%$.

The catastrophic error also affects the scaling relation. It biases both C^{IG} , through the term W_j and n_i in Eq. A1, and C^{Iq} , through the term n_i^2 in Eq. A3. Part of the effect cancels when taking the ratio of the two. The residual error is also of the order $O(f_{\text{cat}})$. Hence from the above order of magnitude estimation, the bias induced by catastrophic error is likely sub-dominant to the major systematical error $\delta f_{ij}^{(c)}$ in the scaling relation. More sophisticated analysis is required to robustly quantify its impact.

4.3. Stochastic galaxy bias

A key assumption in Eq. 10 is the deterministic galaxy bias with respect to the matter distribution. In reality there is stochasticity in galaxy distributions, which can both cause random scatters and systematic shift in the scaling relation. Quantifying its impact is beyond our capability, since the galaxy stochasticity, the intrinsic alignment and correlation between the two are not well understood. For example, the galaxy bias is likely correlated with the strength of the intrinsic alignment, since both depend on the type of galaxies. Nonetheless, there are hopes to control its impact. (1) The galaxy stochasticity can in principle be measured (e.g. Pen 1998; Fan 2003; Bonoli & Pen 2008; Zhang 2008) and modeled (e.g. Baldauf et al. 2009). Measurement and modeling of the intrinsic alignment can be improved too (e.g. Hirata & Seljak 2004; Okumura et al. 2008; Schneider & Bridle 2009). (2) Recently Baldauf et al. (2009) showed that, by proper weighting and modeling, the galaxy stochasticity can be suppressed to 1% level to $k \sim 1h/\text{Mpc}$. Thus there is promise to control the error induced by the galaxy stochasticity in the self-calibration to be $\sim 1\% \times f_{ij}^I$. This error is sub-dominant to other systematical errors, especially the one induced by the scaling relation inaccuracy (§3.3).

⁴ However, some forms of catastrophic error bring better match in the redshift evolution of the integrands of Eq. A1 & A3 and thus can actually improve the accuracy of the scaling relation.

4.4. Cosmological uncertainties

The self-calibration techniques require evaluation of W_{ij} in Eq. 10 and Q in Eq. 15. Both evaluations involve the cosmology-dependent lensing kernel $W_L(z_L, z_G) \propto \Omega_m(1+z_L)\chi_L(1-\chi_L/\chi_G)$. Fortunately, we do not need strong cosmological priors to evaluate it. Ω_m has already been measured to 5% accuracy (Komatsu et al. 2010) and will be measured to below 1% accuracy by Planck.⁵ Stage III BAO and supernova surveys will measure the distance-redshift relation to 1% accuracy (e.g. Albrecht et al. 2006). So if we take these priors, uncertainties in cosmology can at most bias the self-calibration at percent level accuracy, negligible to the identified $\sim 10\%$ scaling relation error in §3.3. We need further investigation to robustly quantify the impact of uncertainties in cosmological parameters.

5. DISCUSSIONS AND SUMMARY

We have proposed a self-calibration technique to eliminate the GI contamination in cosmic shear measurement. It contains two original ingredients. (1) This technique is able to extract the I-g cross correlation from the galaxy density-ellipticity correlation of the same redshift bin in the given lensing survey with photo-z measurement. (2) It then converts this I-g measurement into a measure of the GI correlation through a generic scaling relation. The self-calibration technique has only moderate requirement on the photo-z accuracy and results in little loss of cosmological information. We have performed simple estimation on the performance of this self-calibration technique, which suggests that it can either render the systematical GI contamination into a negligible statistical error, or suppress the GI contamination by a factor of ~ 10 , whichever is larger.

The GI self-calibration can be combined with the photo-z self-calibration (Zhang et al. 2009) for a joint self-calibration against both the GI contamination and the photo-z outliers. This combination does not over-use the information in weak lensing surveys. The GI self-calibration mainly use the galaxy ellipticity-density correlation in the same redshift bin. On the other hand, the

photo-z self-calibration mainly relies on the cross correlation between galaxy ellipticity-density correlation between different redshift bins.

More robust and self-consistent evaluation of the self-calibration (GI and photo-z) performance requires comprehensive analysis of all relevant errors discussed in §3 & 4, and possibly more, along with realistic model of galaxy bias and intrinsic alignment. We expect that our self-calibration technique will still work under this more complicated and more realistic situation, since the method to extract the I-g correlation and the scaling relation between I-g and I-G are robust against the complexities mentioned above. Recently, Joachimi & Bridle (2009); Kirk et al. (2010) proposed simultaneous fittings of cosmological parameters, galaxy bias and intrinsic alignment. Our self-calibration technique can be incorporated in a similar scheme.

Our self-calibration technique only uses the shape-density and density-density measurements in the *same* redshift bin to calibrate the intrinsic alignment. Lensing surveys contain more information on the intrinsic alignment, in the shape-shape correlation of the *same* and between *different* redshift bins, and shape-density correlation between *different* redshift bins. These information has been incorporated by Joachimi & Schneider (2008, 2009); Joachimi & Bridle (2009); Okumura & Jing (2009); Kirk et al. (2010); Shi et al. (2010) to calibrate the intrinsic alignment. These techniques are complementary to each other and shall be combined together for optimal calibration.

Acknowledgments: The author thanks Yipeng Jing and Xiaohu Yang for useful information on galaxy intrinsic ellipticity. The author thanks Gary Bernstein and the anonymous referees for many useful suggestions and comments. This work is supported by the one-hundred-talents program of the Chinese academy of science (CAS), the national science foundation of China (grant No. 10821302 & 10973027) and the 973 program grant No. 2007CB815401.

⁵ http://www.rssd.esa.int/index.php?project=PLANCK&page=perf_top

REFERENCES

- The Dark Energy Task Force Report. Andreas Albrecht, et al. arXiv:astro-ph/0609591
- Bacon, D. J., Refregier, A. R., & Ellis, R. S. 2000, MNRAS, 318, 625
- Baldauf, T., Smith, R. E., Seljak, U., & Mandelbaum, R. 2009, arXiv:0911.4973
- Bartelmann, M. 1995, A&A, 298, 661
- Benjamin, J., Van Waerbeke, L., Ménard, B., & Kilbinger, M. 2010, arXiv:1002.2266
- Bernstein, G. M. 2009, Astrophys. J. , 695, 652
- Bernstein, G., & Huterer, D. 2009, arXiv:0902.2782
- Bonoli, S., & Pen, U.-L. 2008, arXiv:0810.0273
- Bridle, S., & King, L. 2007, New Journal of Physics, 9, 444
- Brown, M. L., Taylor, A. N., Hambly, N. C., & Dye, S. 2002, MNRAS, 333, 501
- Catelan, P., Kamionkowski, M., & Blandford, R. D. 2001, MNRAS, 320, L7
- Crittenden, R. G., Natarajan, P., Pen, U.-L., & Theuns, T. 2001, Astrophys. J. , 559, 552
- Crittenden, R. G., Natarajan, P., Pen, U.-L., & Theuns, T. 2002, Astrophys. J. , 568, 20
- Croft, R. A. C., & Metzler, C. A. 2000, Astrophys. J. , 545, 561
- Fan, Z. 2003, Astrophys. J. , 594, 33
- Fu, L., et al. 2008, A&A, 479, 9
- Guo, H., & Jing, Y. P. 2009, Astrophys. J. , 702, 425
- Hamana, T. 2001, MNRAS, 326, 326
- Hearin, A. P., Zentner, A. R., Ma, Z., & Huterer, D. 2010, arXiv:1002.3383
- Heavens, A., Refregier, A., & Heymans, C. 2000, MNRAS, 319, 649
- Heymans, C., & Heavens, A. 2003, MNRAS, 339, 711
- Heymans, C., Brown, M., Heavens, A., Meisenheimer, K., Taylor, A., & Wolf, C. 2004, MNRAS, 347, 895
- Heymans, C., White, M., Heavens, A., Vale, C., & van Waerbeke, L. 2006, MNRAS, 371, 750
- Hirata, C. M., et al. 2004, MNRAS, 353, 529
- Hirata, C. M., & Seljak, U. 2004, Phys. Rev. D , 70, 063526
- Hirata, C. M., Mandelbaum, R., Ishak, M., Seljak, U., Nichol, R., Pimbblet, K. A., Ross, N. P., & Wake, D. 2007, MNRAS, 381, 1197
- Hoekstra, H., & Jain, B. 2008, arXiv:0805.0139
- Hu, W., & Jain, B. 2004, Phys. Rev. D , 70, 043009
- Jing, Y. P. 2002, MNRAS, 335, L89
- Jing, Y. P., Zhang, P., Lin, W. P., Gao, L., & Springel, V. 2006, ApJ, 640, L119

- Joachimi, B., & Schneider, P. 2008, *A&A*, 488, 829
 Joachimi, B., & Schneider, P. 2009, arXiv:0905.0393
 Joachimi, B., & Bridle, S. L. 2009, arXiv:0911.2454
 Jovel, S., et al. 2009, arXiv:0902.0625
 Kaiser, N., Wilson, G., & Luppino, G. A. 2000, arXiv:astro-ph/0003338
 Kang, X., van den Bosch, F. C., Yang, X., Mao, S., Mo, H. J., Li, C., & Jing, Y. P. 2007, *MNRAS*, 378, 1531
 King, L., & Schneider, P. 2002, *A&A*, 396, 411
 King, L. J., & Schneider, P. 2003, *A&A*, 398, 23
 Kirk, D., Bridle, S., & Schneider, M. 2010, arXiv:1001.3787
 Komatsu, E., et al. 2009, *ApJS*, 180, 330
 Komatsu, E., et al. 2010, arXiv: 1010.4538
 Lee, J., & Pen, U.-L. 2000, *ApJ*, 532, L5
 Lee, J., & Pen, U.-L. 2001, *Astrophys. J.*, 555, 106
 Lee, J., & Pen, U.-L. 2002, *ApJ*, 567, L111
 Lee, J., & Pen, U.-L. 2007, *ApJ*, 670, L1
 Mackey, J., White, M., & Kamionkowski, M. 2002, *MNRAS*, 332, 788
 Mandelbaum, R., Hirata, C. M., Ishak, M., Seljak, U., & Brinkmann, J. 2006, *MNRAS*, 367, 611
 Munshi, D., Valageas, P., van Waerbeke, L., & Heavens, A. 2008, *Physics Reports*, 462, 67
 Newman, J. A. 2008, *Astrophys. J.*, 684, 88
 Okumura, T., Jing, Y. P., & Li, C. 2008, arXiv:0809.3790
 Okumura, T., & Jing, Y. P. 2009, *ApJ*, 694, L83
 Pen, U.-L. 1998, *Astrophys. J.*, 504, 601
 Pen, U.-L., Lee, J., & Seljak, U. 2000, *ApJ*, 543, L107
 Refregier, A. 2003, *Annual Review of Astronomy & Astrophysics*, 41, 645
 Rudd, D. H., Zentner, A. R., & Kravtsov, A. V. 2008, *Astrophys. J.*, 672, 19
 Schneider, P., King, L., & Erben, T. 2000, *A&A*, 353, 41
 Schneider, M., Knox, L., Zhan, H., & Connolly, A. 2006, *Astrophys. J.*, 651, 14
 Schneider, M. D., & Bridle, S. 2009, arXiv:0903.3870
 Scranton, R., et al. 2005, *Astrophys. J.*, 633, 589
 Sheldon, E. S., et al. 2004, *Astronomical Journal*, 127, 2544
 Shi, X., Joachimi, B., & Schneider, P. 2010, arXiv:1002.0693
 Stebbins, A. 1996, arXiv:astro-ph/9609149
 Szapudi, I., & Pan, J. 2004, *Astrophys. J.*, 602, 26
 Takada, M., & White, M. 2004, *ApJ*, 601, L1
 Van Waerbeke, L., et al. 2000, *A&A*, 358, 30
 Wang, Y., Park, C., Yang, X., Choi, Y.-Y., & Chen, X. 2008, arXiv:0810.3359
 White, M. 2004, *Astroparticle Physics*, 22, 211
 Wittman, D. M., Tyson, J. A., Kirkman, D., Dell’Antonio, I., & Bernstein, G. 2000, *Nature (London)*, 405, 143
 Yang, X., Mo, H. J., & van den Bosch, F. C. 2003, *MNRAS*, 339, 1057
 Yang, X., van den Bosch, F. C., Mo, H. J., Mao, S., Kang, X., Weinmann, S. M., Guo, Y., & Jing, Y. P. 2006, *MNRAS*, 369, 1293
 Zhan, H., & Knox, L. 2004, *ApJ*, 616, L75
 Zhan, H., & Knox, L. 2006, arXiv:astro-ph/0611159
 Zhang, P. 2008, arXiv:0802.2416
 Zhang, P., Pen, U.-L., & Bernstein, G. 2010, *MNRAS*, 405, 359 [arXiv:0910.4181]
 Zhang, P. 2010, *MNRAS letters*, in press. arXiv:1003.5219.
 Zhang, Y., Yang, X., Faltenbacher, A., Springel, V., Lin, W., & Wang, H. 2009, *Astrophys. J.*, 706, 747
 Zheng, Z., et al. 2005, *Astrophys. J.*, 633, 791

APPENDIX

A: THE SCALING RELATION

We derive the scaling relation (Eq. 10) under the Limber approximation. Under this approximation, the 2D GI angular cross correlation power spectrum between the i -th and j -th redshift bins is related to the 3D matter-intrinsic alignment cross correlation power spectrum $\Delta_{mI}^2(k, z)$ by

$$\frac{\ell^2}{2\pi} C_{ij}^{IG}(\ell) = \frac{\pi}{\ell} \int_0^\infty \Delta_{mI}^2 \left(k = \frac{\ell}{\chi(z)}, z \right) W_j(z) \chi(z) \bar{n}_i(z) dz. \quad (\text{A1})$$

Here,

$$W_j(z_L) \equiv \int_0^\infty W_L(z_L, z_G) \bar{n}_j(z_G) dz_G. \quad (\text{A2})$$

As a reminder, $\bar{n}_i(z)$ is the true redshift distribution of galaxies in the i -th redshift bin and $W_L(z_L, z_G)$ is the lensing kernel. The integral limit runs from zero to infinite, to take into account the photo- z errors. On the other hand, the 2D angular power spectrum between the intrinsic alignment and galaxy number density in the i -th redshift bin is

$$\frac{\ell^2}{2\pi} C_{ii}^{Ig}(\ell) = \frac{\pi}{\ell} \int_0^\infty \Delta_{gI}^2 \left(k = \frac{\ell}{\chi(z)}, z \right) n_i^2(z) \chi(z) \frac{dz}{d\chi} dz = b_i(\ell) \frac{\pi}{\ell} \int_0^\infty \Delta_{mI}^2 \left(k = \frac{\ell}{\chi(z)}, z \right) n_i^2(z) \chi(z) \frac{dz}{d\chi} dz. \quad (\text{A3})$$

$\Delta_{gI}^2(k, z)$ is the 3D galaxy-galaxy intrinsic alignment power spectrum. In the last relation we have adopted a deterministic galaxy bias $b_g(k, z)$ with respect to matter distribution and thus $\Delta_{gI}^2(k, z) = b_g(k, z) \Delta_{mI}^2(k, z)$. $b_i(\ell)$ is defined by the above equation. It is the average of $b_g(k = \ell/\chi, z)$ over the redshift bin. As long as $b_g(k, z)$ does not change dramatically, we have $b_i(\ell) = b_g(k = \ell/\chi_i, \bar{z}_i)$, to a good approximation.

In the limit that the true redshift distribution of galaxies in the i -th redshift bin is narrow, Δ_{mI}^2 (Δ_{gI}^2) changes slowly and can be approximated as $\Delta_{mI}^2(k = \ell/\chi_i, \bar{z}_i)$ ($\Delta_{gI}^2(k = \ell/\chi_i, \bar{z}_i)$). We then have the following approximations,

$$\frac{\ell^2}{2\pi} C_{ij}^{IG}(\ell) \simeq \frac{\pi}{\ell} \Delta_{mI}^2 \left(\frac{\ell}{\chi_i}, \bar{z}_i \right) W_{ij} \chi_i, \quad (\text{A4})$$

and

$$\frac{\ell^2}{2\pi} C_{ii}^{Ig}(\ell) \simeq b_i(\ell) \frac{\pi}{\ell} \Delta_{mI}^2 \left(\frac{\ell}{\chi_i}, \bar{z}_i \right) \frac{\chi_i}{\Delta_i}. \quad (\text{A5})$$

The quantity W_{ij} and Δ_i are already defined by Eq. 11 & 12. Based on the above two equations, we derive Eq. 10, whose accuracy is quantified in §3.3.

B: EVALUATING THE Q PARAMETER

To derive the relation between $C_{ii}^{Gg}|_S$ and C_{ii}^{Gg} , namely, $Q \equiv C_{ii}^{Gg}|_S / C_{ii}^{Gg}$, we will begin with the real space angular correlation function. We denote the angular correlation function between the shear at z_G^P and galaxies at z_g^P as $w^{Gg}(\theta; z_G^P, z_g^P)$. Its average over the distribution of galaxies in the i -th redshift bin is

$$\begin{aligned} w_{ii}^{Gg}(\theta) &= \int_{\bar{z}_i - \Delta z_i/2}^{\bar{z}_i + \Delta z_i/2} dz_G^P \int_{\bar{z}_i - \Delta z_i/2}^{\bar{z}_i + \Delta z_i/2} dz_g^P w^{Gg}(\theta; z_G^P, z_g^P) n_i^P(z_G^P) n_i^P(z_g^P) dz_G^P dz_g^P \\ &= \int_{\bar{z}_i - \Delta z_i/2}^{\bar{z}_i + \Delta z_i/2} dz_G^P \int_{\bar{z}_i - \Delta z_i/2}^{\bar{z}_i + \Delta z_i/2} dz_g^P \int_0^\infty dz_G \int_0^\infty dz_g [w^{Gg}(\theta; z_G, z_g) p(z_G|z_G^P) p(z_g|z_g^P) n_i^P(z_G^P) n_i^P(z_g^P)] . \end{aligned} \quad (B1)$$

Here, $p(z|z^P)$ is the photo- z PDF. As a reminder, we have normalized such that

$$\int_{\bar{z}_i - \Delta z_i/2}^{\bar{z}_i + \Delta z_i/2} dz^P n_i^P(z^P) = \int_0^\infty n_i(z) dz = 1 .$$

Since

$$w^{Gg}(\theta; z_G, z_g) = \int \langle \delta_m(\theta'; z_L) \delta_g(\theta' + \theta; z_g) \rangle W_L(z_L, z_G) dz_L , \quad (B2)$$

where $\langle \dots \rangle$ denotes the ensemble average and in practice denotes equivalently the average over θ' (the ergodicity assumption), we have

$$\begin{aligned} w_{ii}^{Gg}(\theta) &= \int_{\bar{z}_i - \Delta z_i/2}^{\bar{z}_i + \Delta z_i/2} dz_G^P \int_{\bar{z}_i - \Delta z_i/2}^{\bar{z}_i + \Delta z_i/2} dz_g^P \int_0^\infty dz_G \int_0^\infty dz_g \int_0^\infty dz_L \\ &\quad \times \left[\langle \delta_m(\theta'; z_L) \delta_g(\theta' + \theta; z_g) \rangle W_L(z_L, z_G) p(z_G|z_G^P) p(z_g|z_g^P) n_i^P(z_G^P) n_i^P(z_g^P) \right] \\ &= \int_0^\infty dz_L \int_0^\infty dz_g \left[\langle \delta_m(\theta'; z_L) \delta_g(\theta' + \theta; z_g) \rangle W_i(z_L) n_i(z_g) \right] . \end{aligned} \quad (B3)$$

Notice that the lensing kernel $W_L(z_L, z_G) = 0$ when $z_L \geq z_G$. The average over all pairs with $z_G^P < z_g^P$ gives the other correlation function,

$$w_{ii}^{Gg}|_S(\theta) = \int \langle \delta_m(\theta'; z_L) \delta_g(\theta' + \theta; z_g) \rangle W_i(z_L) n_i(z_g) dz_L dz_g \eta(z_L, z_g) . \quad (B4)$$

Here,

$$\eta(z_L, z_g) = \frac{2 \int_{\bar{z}_i - \Delta z_i/2}^{\bar{z}_i + \Delta z_i/2} dz_G^P \int_{\bar{z}_i - \Delta z_i/2}^{\bar{z}_i + \Delta z_i/2} dz_g^P \int_0^\infty dz_G W_L(z_L, z_G) p(z_G|z_G^P) p(z_g|z_g^P) S(z_G^P, z_g^P) n_i^P(z_G^P) n_i^P(z_g^P)}{\int_{\bar{z}_i - \Delta z_i/2}^{\bar{z}_i + \Delta z_i/2} dz_G^P \int_{\bar{z}_i - \Delta z_i/2}^{\bar{z}_i + \Delta z_i/2} dz_g^P \int_0^\infty dz_G W_L(z_L, z_G) p(z_G|z_G^P) p(z_g|z_g^P) n_i^P(z_G^P) n_i^P(z_g^P)} , \quad (B5)$$

where the selection function $S(z_G^P, z_g^P) = 1$ if $z_G^P < z_g^P$ and $S(z_G^P, z_g^P) = 0$ otherwise. The factor 2 comes from the relation

$$\frac{\int_{\bar{z}_i - \Delta z_i/2}^{\bar{z}_i + \Delta z_i/2} dz_G^P \int_{\bar{z}_i - \Delta z_i/2}^{\bar{z}_i + \Delta z_i/2} dz_g^P p(z_G|z_G^P) p(z_g|z_g^P) n_i^P(z_G^P) n_i^P(z_g^P)}{\int_{\bar{z}_i - \Delta z_i/2}^{\bar{z}_i + \Delta z_i/2} dz_G^P \int_{\bar{z}_i - \Delta z_i/2}^{\bar{z}_i + \Delta z_i/2} dz_g^P p(z_G|z_G^P) p(z_g|z_g^P) S(z_G^P, z_g^P) n_i^P(z_G^P) n_i^P(z_g^P)} = 2 . \quad (B6)$$

The power spectra C_{ii}^{Gg} and $C_{ii}^{Gg}|_S$ are the Fourier transform of w_{ii}^{Gg} and $w_{ii}^{Gg}|_S$, respectively. To evaluate these power spectra, we again follow the Limber approximation, which states that the dominant correlation signal comes from $z_L = z_g$. We then have

$$\frac{\ell^2 C_{ii}^{Gg}(\ell)}{2\pi} = \frac{\pi}{\ell} \int_0^\infty \Delta_{mg}^2 \left(k = \frac{\ell}{\chi(z)}, z \right) \chi(z) W_i(z) n_i(z) dz , \quad (B7)$$

$$\frac{\ell^2 C_{ii}^{Gg}|_S(\ell)}{2\pi} = \frac{\pi}{\ell} \int_0^\infty \Delta_{mg}^2 \left(k = \frac{\ell}{\chi(z)}, z \right) W_i(z) \chi(z) n_i(z) \eta(z, z_g = z) dz . \quad (B8)$$

The quantity that we want to evaluate is $Q(\ell) \equiv C_{ii}^{Gg}|_S(\ell) / C_{ii}^{Gg}(\ell)$. Since it is the ratio of the two power spectra, in which Δ_{mg}^2 , W_i and n_i roughly cancel, to the first order, $Q \simeq \eta$. The value of η is determined by the relative contribution to C^{Gg} from pairs with $z_G^P < z_g^P$ and pairs with $z_G^P > z_g^P$. If the two sets have the same contribution, $\eta = 1$ and $Q = 1$. In the limit $\sigma_P \gg \Delta z$, the contribution from the pair with $z_G^P < z_g^P$ to C_{ii}^{Gg} approaches to that of the pair with $z_G^P > z_g^P$. So we have $\eta \rightarrow 1$ and $Q \rightarrow 1$. In this limiting case, we will be no longer able to use this weighting scheme to separate C^{Gg} and C^{Ig} . On the other hand, if $\sigma_P \ll \Delta z$, the pair with $z_G^P < z_g^P$ virtually does not contribute to C^{Gg} , we will have $\eta \rightarrow 0$ and $Q \rightarrow 0$, as would happen for spectroscopic redshifts. As long as Q deviates significantly from unity, C_{ii}^{Ig} can be separated from C_{ii}^{Gg} . For a LSST-like survey with $\Delta z = 0.2$ and $\sigma_P = 0.05(1+z)$, we numerically evaluate $\eta(z, z_g)$ and $Q(l)$. We find that $Q \sim 1/2$ (Fig. 2). The significant deviation of Q from unity is the manifestation of relatively large photo- z error σ_P , across which the lensing efficiency changes dramatically.

C: THE STATISTICAL ERROR IN EXTRACTING C_{II}^{Ig}

For the convenience, we will work on the pixel space to derive the statistical error in extracting C_{ii}^{Ig} from the galaxy shape (ellipticity)-density measurement in the i -th photo- z bin. For a given redshift bin, we first pixelize the data into sufficiently fine (and uniform) pixels of photo- z and angular position. Each pixel, with label α , has a corresponding photo- z z_α^P and corresponding angular position $\vec{\theta}_\alpha$. Each pixel also has a measured overdensity $\delta_\alpha + \delta_\alpha^N$ and a measured “shear”, $\kappa_\alpha + I_\alpha + \kappa_\alpha^N$. Here, the superscript “N” denotes the measurement noise, e.g., the shot noise. In total, there are N_P pixels. Following the definition of the angular power spectrum, we have

$$C^{(2)}(\ell) = N_P^{-2} \sum_{\alpha\beta} [\delta_\alpha + \delta_\alpha^N] [\kappa_\beta + I_\beta + \kappa_\beta^N] \exp \left[i\vec{\ell} \cdot (\vec{\theta}_\alpha - \vec{\theta}_\beta) \right],$$

$$C^{(2)}(\ell)|_S = 2N_P^{-2} \sum_{\alpha\beta} [\delta_\alpha + \delta_\alpha^N] [\kappa_\beta + I_\beta + \kappa_\beta^N] \exp \left[i\vec{\ell} \cdot (\vec{\theta}_\alpha - \vec{\theta}_\beta) \right] \times S_{\alpha\beta}. \quad (C1)$$

Here, $S_{\alpha\beta} = 1$ when $z_\alpha^P > z_\beta^P$ and vanishes otherwise. In the limit that $N_P \gg 1$, $\sum_{\alpha\beta} S_{\alpha\beta} = N_P^2/2$. Namely, the average $\overline{S_{\alpha\beta}} = 1/2$.

The C^{Ig} measurement error, from Eq. 15, is

$$\begin{aligned} \delta C^{Ig} &= \frac{1}{(1-Q)} N_P^{-2} \sum_{\alpha\beta} \exp \left[i\vec{\ell} \cdot (\vec{\theta}_\alpha - \vec{\theta}_\beta) \right] [(\delta_\alpha + \delta_\alpha^N)(\kappa_\beta + I_\beta + \kappa_\beta^N)(2S_{\alpha\beta} - Q) - (1-Q)\delta_\alpha I_\beta] \\ &= \frac{1}{(1-Q)} N_P^{-2} \sum_{\alpha\beta} \exp \left[i\vec{\ell} \cdot (\vec{\theta}_\alpha - \vec{\theta}_\beta) \right] [(\delta_\alpha(\kappa_\beta + \kappa_\beta^N) + \delta_\alpha^N(\kappa_\beta + I_\beta + \kappa_\beta^N)) (2S_{\alpha\beta} - Q)]. \end{aligned} \quad (C2)$$

The last expression has utilized the relation $\overline{S_{\alpha\beta}} = 1/2$ and the fact that the density-intrinsic alignment correlation does not depend on the ordering along the line-of-sight of galaxy pairs. The rms error is

$$\begin{aligned} (\Delta C^{Ig})^2 &= \frac{1}{(1-Q)^2} N_P^{-4} \sum_{\alpha\beta\rho\sigma} \exp \left[i\vec{\ell} \cdot (\vec{\theta}_\alpha - \vec{\theta}_\beta) \right] \exp \left[-i\vec{\ell} \cdot (\vec{\theta}_\rho - \vec{\theta}_\sigma) \right] (2S_{\alpha\beta} - Q)(2S_{\rho\sigma} - Q) \\ &\quad \times \langle [(\delta_\alpha(\kappa_\beta + \kappa_\beta^N) + \delta_\alpha^N(\kappa_\beta + I_\beta + \kappa_\beta^N)) [(\delta_\rho(\kappa_\sigma + \kappa_\sigma^N) + \delta_\rho^N(\kappa_\sigma + I_\sigma + \kappa_\sigma^N))] \rangle. \end{aligned}$$

Here, $\langle \dots \rangle$ denotes the ensemble average. To proceed, we adopt a common simplification in the lensing error analysis, namely the Wick theorem for 4-point correlation (which holds strictly for Gaussian field),

$$\langle ABCD \rangle = \langle AB \rangle \langle CD \rangle + \langle AC \rangle \langle BD \rangle + \langle BC \rangle \langle AD \rangle; \quad A, B, C, D \in \delta, \delta^N, \kappa, \kappa^N, I.$$

Plug the above equation in and keep all non-vanishing terms, we then have

$$\begin{aligned} (\Delta C^{Ig})^2 &= \frac{1}{(1-Q)^2} N_P^{-4} \sum_{\alpha\beta\rho\sigma} \exp \left[i\vec{\ell} \cdot (\vec{\theta}_\alpha - \vec{\theta}_\beta) \right] \exp \left[-i\vec{\ell} \cdot (\vec{\theta}_\rho - \vec{\theta}_\sigma) \right] (2S_{\alpha\beta} - Q)(2S_{\rho\sigma} - Q) \\ &\quad \times [\langle \delta_\alpha \delta_\rho \rangle \langle \kappa_\beta \kappa_\sigma \rangle + \langle \delta_\alpha \delta_\rho \rangle \langle \kappa_\beta^N \kappa_\sigma^N \rangle + \langle \delta_\alpha^N \delta_\rho^N \rangle \langle (\kappa_\beta + I_\beta)(\kappa_\sigma + I_\sigma) \rangle + \langle \delta_\alpha^N \delta_\rho^N \rangle \langle \kappa_\beta^N \kappa_\sigma^N \rangle]. \end{aligned} \quad (C3)$$

Notice that the sum over $\langle \delta_\alpha \kappa_\beta \rangle \langle \delta_\rho \kappa_\sigma \rangle$ terms vanishes, resulting from the definition of Q . The sum over $\langle \delta_\alpha \kappa_\sigma \rangle \langle \delta_\rho \kappa_\beta \rangle$ terms also vanishes, due to the mis-match between the Fourier phases (e.g. the one $\propto \vec{\theta}_\alpha + \vec{\theta}_\sigma$) and the angular dependence of the correlation functions (e.g. $\langle \delta_\alpha \kappa_\sigma \rangle = w_{gG}(\vec{\theta}_\alpha - \vec{\theta}_\sigma)$).

Correlation functions in Eq. C3 depend on the absolute pair separation, but not on the relative pair orientation. For example, $\langle \delta_\alpha \delta_\rho \rangle = \langle \delta_\rho \delta_\alpha \rangle = w_g(|\vec{\theta}_\alpha - \vec{\theta}_\rho|)$, whose Fourier transform is the galaxy angular power spectrum C^{gg} . This allows us to do the sums above analytically and obtain the final expression of the rms error for a single ℓ mode

$$(\Delta C^{Ig})^2 = C^{gg} C^{GG} + [C^{gg} C^{GG,N} + C^{gg,N} (C^{GG} + C^{II})] \left[1 + \frac{1}{3(1-Q)^2} \right] + C^{gg,N} C^{GG,N} \left[1 + \frac{1}{(1-Q)^2} \right]. \quad (C4)$$

In the above expression, we have used the fact that noises only correlate at zero-lag ($\langle \kappa_\beta^N \kappa_\sigma^N \rangle \propto \delta_{\beta\sigma}$ and $\langle \delta_\alpha^N \delta_\rho^N \rangle \propto \delta_{\alpha\rho}$) and the following relations,

$$\begin{aligned} \frac{1}{N_P^4} \sum_{\alpha\beta\rho\sigma} (2S_{\alpha\beta} - Q)(2S_{\rho\sigma} - Q) &\simeq (1-Q)^2, \\ \frac{1}{N_P^3} \sum_{\alpha\beta\rho} (2S_{\alpha\beta} - Q)(2S_{\rho\beta} - Q) &\simeq (1-Q)^2 + \frac{1}{3}, \\ \frac{1}{N_P^2} \sum_{\alpha\beta} (2S_{\alpha\beta} - Q)^2 &\simeq (1-Q)^2 + 1. \end{aligned}$$

In the above relations, we have neglected terms of the order $O(1/N_P)$ and higher, since the number of pixels $N_P \gg 1$.

Each term in the r.h.s of Eq. C4 has specific physical meaning and hence deserves brief explanation.

- The first term $C^{gg}C^{GG}$ is the cosmic variance arising from the lensing and galaxy density fluctuations. The Q dependence drops out, since both $C^{(2)}$ and $C^{(2)}|_S$ sample the same cosmic volume and share the identical (fractional) cosmic variance from this term.

$C^{gg}C^{GG}$ is a familiar term in the cosmic variance of the ordinary galaxy-galaxy lensing power spectrum. However, the other familiar term, $C^{gG,2}$, does not show up here. This again is caused by the fact that both $C^{(2)}$ and $C^{(2)}|_S$ sample the same cosmic volume and the cosmic variances inducing $C^{gG,2}$ cancel in the estimator Eq. 15.

- The last term $C^{gg,N}C^{GG,N}[1 + 1/(1 - Q)^2]$ is the contribution from the shot noise in the galaxy distribution and random shape shot noise in shear measurement. The Q dependence can be understood as follows. Such error in $C^{(2)}$ has two contributions, δC_A from pairs with $z_g^P > z_G^P$ and δC_B from pairs with $z_g^P \leq z_G^P$. The total error is $(\delta C_A + \delta C_B)/2$. Since they come from different pairs, these two errors are uncorrelated ($\langle \delta C_A \delta C_B^* \rangle = 0$), but they have the same dispersion $\langle |\delta C_A|^2 \rangle = \langle |\delta C_B|^2 \rangle = 2C^{gg,N}C^{GG,N}$. The factor 2 here provides the correct rms noise in $C^{(2)}$, which is $C^{gg,N}C^{GG,N}$. Clearly the shot noise error in $C^{(2)}|_S$ is δC_A . Plug the above relations into Eq. 15, we find that the shot noise contribution is indeed the last term in Eq. C4. Unlike the cosmic variance term, which does not rely on Q , the shot noise term blows up when $Q \rightarrow 1$. This corresponds to the case that the photo- z error is too large to provide any useful information and thus we are no longer able to separate the Ig contribution from the Gg contribution.
- The middle term is the cross talk between cosmic variance and shot noise. One can find similar terms in usual cross correlation statistical error analysis.

Interestingly, when $(1 - Q)^2 = 1/3$ and when $C^{II} \ll C^{GG}$, Eq. C4 reduces to

$$(\Delta C^{Ig})^2 \simeq (C^{gg} + 2C^{gg,N})(C^{GG} + 2C^{GG,N}), \quad \text{when } Q \sim 1 - \sqrt{1/3} = 0.423. \quad (\text{C5})$$

This expression is identical to the usual expression of cross correlation statistical error, except for the factor 2.